Applications of atomic layer deposition in solar cells

2015 Nanotechnology 26 064001

(http://iopscience.iop.org/0957-4484/26/6/064001)

OPEN ACCESS
IOP Publishing
Nanotechnology

Nanotechnology **26** (2015) 064001 (13pp)
doi:10.1088/0957-4484/26/6/064001

Review

Applications of atomic layer deposition in solar cells

Wenbin Niu[1], Xianglin Li[1], Siva Krishna Karuturi[2], Derrick Wenhui Fam[1], Hongjin Fan[3], Santosh Shrestha[2], Lydia Helena Wong[1] and Alfred Iing Yoong Tok[1]

[1] School of Materials Science and Engineering, Nanyang Technological University, 50 Nanyang Avenue, 639798, Singapore
[2] School of Photovoltaic and Renewable Energy Engineering, University of New South Wales, Sydney, NSW 2052, Australia
[3] Division of Physics and Applied Physics, School of Physical and Mathematical Sciences, Nanyang Technological University, 21 Nanyang Link, 637371, Singapore

E-mail: MIYTok@ntu.edu.sg

Received 25 June 2014, revised 17 September 2014
Accepted for publication 29 September 2014
Published 20 January 2015

Abstract

Atomic layer deposition (ALD) provides a unique tool for the growth of thin films with excellent conformity and thickness control down to atomic levels. The application of ALD in energy research has received increasing attention in recent years. In this review, the versatility of ALD in solar cells will be discussed. This is specifically focused on the fabrication of nanostructured photoelectrodes, surface passivation, surface sensitization, and band-structure engineering of solar cell materials. Challenges and future directions of ALD in the applications of solar cells are also discussed.

Keywords: atomic layer deposition, solar cells, surface passivation, surface sensitization, band-structure engineering

(Some figures may appear in colour only in the online journal)

1. Introduction

Atomic layer deposition (ALD) is a low-temperature, vacuum, vapor-phase thin film growth technique that allows precise control in film thickness on an atomic scale and uniformity. It distinguishes itself from chemical vapor deposition (CVD) in that the precursors in an ALD process are injected into the reaction chamber in sequenced deposition cycles [1]. In this way, the precursors will not pre-react in the chamber before anchoring the substrate surface. With ALD, nearly 100% step coverage is possible especially for most binary oxides, but also depends on the gas flow mechanism. Recent attention to ALD is being focused on the deposition of smooth and uniform thin (from 10 down to 1 nm) films on non-planar three-dimensional (3D) structures. As summarized by several recent reviews and books, ALD has become a popular and powerful tool for the template-assisted fabrication of complex nanostructures and tailoring of physical properties of nanomaterials [1, 2].

For applications in energy-related research, the reader is encouraged to refer a few recent review articles [3–6]. Application in improving the cyclic stability and energy density of electrochemical energy storage devices (lithium-ion batteries and supercapacitors) [5, 7, 8], will be discussed in another review of this special issue. In this review, our focus is directed on solar cells, including dye-sensitized solar cells (DSSCs), quantum dot sensitized solar cells, organic–inorganic hybrid solar cells, thin-film solar cells (Si and Cu(In,Ga)Se_2 (CIGS)), and photoelectrochemical (PEC) cells. The role of ALD thin

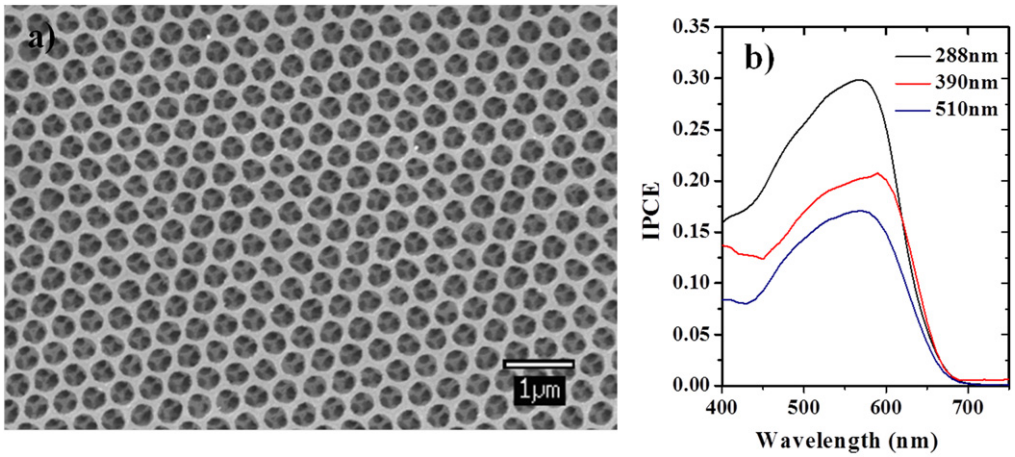

Figure 1. (a) FESEM image of TiO_2 inverse opal based on 510 nm polystyrene opals. (b) Incident photon to current conversion efficiency (IPCE) of DSSCs with TiO_2 inverse opal based electrodes of different pore sizes [17]. Copyright 2011 Royal Society of Chemistry.

films in solar cell functions can be classified into three major categories: (1) fabrication of nanostructured active electrodes or charge transporters (e.g., ZnO, ZnS, TiO_2, Fe_2O_3, Cu_2O); (2) forming heterojunction (e.g., AlZnO, TiO_2, CdS or CdSe); (3) inert surface passivation of trap states (e.g., Al_2O_3, HfO_2); and (4) catalytic noble metals (e.g., Pt, Pd, Ru, Ir, and composite metals) [9].

This article discusses typical application of ALD in solar cells. It starts with the fabrication of nanostructured electrodes, followed by electrode surface passivation, electrode surface sensitization by quantum dots and metal nanoparticles, and finally band-structure engineering in dye-sensitized and CIGS solar cells.

2. Nanostructured cell electrodes fabricated via ALD

2.1. Inverse opal-based photoelectrode

Inverse opal is a replicated shell structure of face-centered-cubic opal, with high specific surface area and porosity (74% void volume). The periodical 3D inverse opal exhibits photonic crystal properties, thereby providing additional avenues to enhance light–matter interactions by controlling the propagation of light via mirror reflections, slow photons, and surface resonant modes [10–13]. As such, the inverse opal structure is an ideal electrode architecture for energy conversion applications. TiO_2 inverse opals have attracted a lot of attention in DSSCs as optical elements that impart the light management within device. Mallouk *et al* first reported dual-layer photoanode structure, with a bottom 3D TiO_2 inverse opal film to selectively reflect the photons onto the conventional nanocrystalline TiO_2 top layer and enhance light harvesting [13]. The subsequent studies by Mihi and Miguez *et al* extensively analyzed the enhancement mechanism [14, 15]. A challenging issue here is the fabrication of high quality TiO_2 inverse opal. When synthesized using sol–gel hydrolysis or nanoparticle infiltration of opal template to form an inverse opal structure, it is very difficult to achieve full infiltration, which deteriorate optoelectrical properties of the electrodes.

Karuturi *et al* established the effectiveness of ALD technique to fabricate inverse opals by investigating the mechanism of template filling using opal structures. Controlled filling of opal templates with close to theoretical filling was demonstrated [16]. Subsequently, as-fabricated high quality inverse opals with different pore sizes on fluorine-doped tin-oxide-coated glass substrate were studied as a photoanode for DSSCs application as shown in figure 1. These structures were found possessing several advantages as conformality and high filling fractions ensure robust interfacial contact with the substrate, thereby providing good electron transport paths. The power conversion efficiencies of 2.22%, 1.81% and 1.42% (AM1.5) were achieved using electrodes with pore sizes of 288 nm, 390 nm and 510 nm, respectively [17]. When compared to the conventional nanocrystalline TiO_2 type of photoanode in DSSCs, inverse opal electrode showed weaker absorption due to its low surface area for dye loading. Tetreault *et al* resolved this issue by filling the voids of inverse opal (Al/ZnO, TiO_2) fabricated using ALD with high surface area nanocrystalline TiO_2. Highest power conversion efficiency of 4.9% was reported using non-optimized electrodes due to enhanced surface area from nanocrystalline TiO_2 and improved electron mobility from highly conductive Al/ZnO layer [12].

Very similar to DSSCs, PEC splitting of water into H_2 and O_2 by using sunlight holds promise to convert intermittent solar energy into stable and storable chemical fuel. Crucial to the light harvesting and conversion efficiency of a PEC cell is a nanostructured photoanode where the incident photons are captured, electron hole pairs are generated and the subsequent electron transfer takes place [18–20]. Inverse opal based electrodes holds promise as they possess several favorable intrinsic characteristics for efficient solar energy conversion such as direct electron transport pathways for longer electron diffusion length, light scattering to promote the light harvesting ability by confining the light within the cell and intimate contact with the electrolyte for faster oxidation and reduction reaction kinetics.

Cheng and Karuturi *et al* investigated CdS quantum dots sensitized TiO_2 inverse opal electrodes (figure 2(a)) for the first time for PEC hydrogen generation. While TiO_2 inverse opals with three different pore sizes of 288, 510 and 900 nm

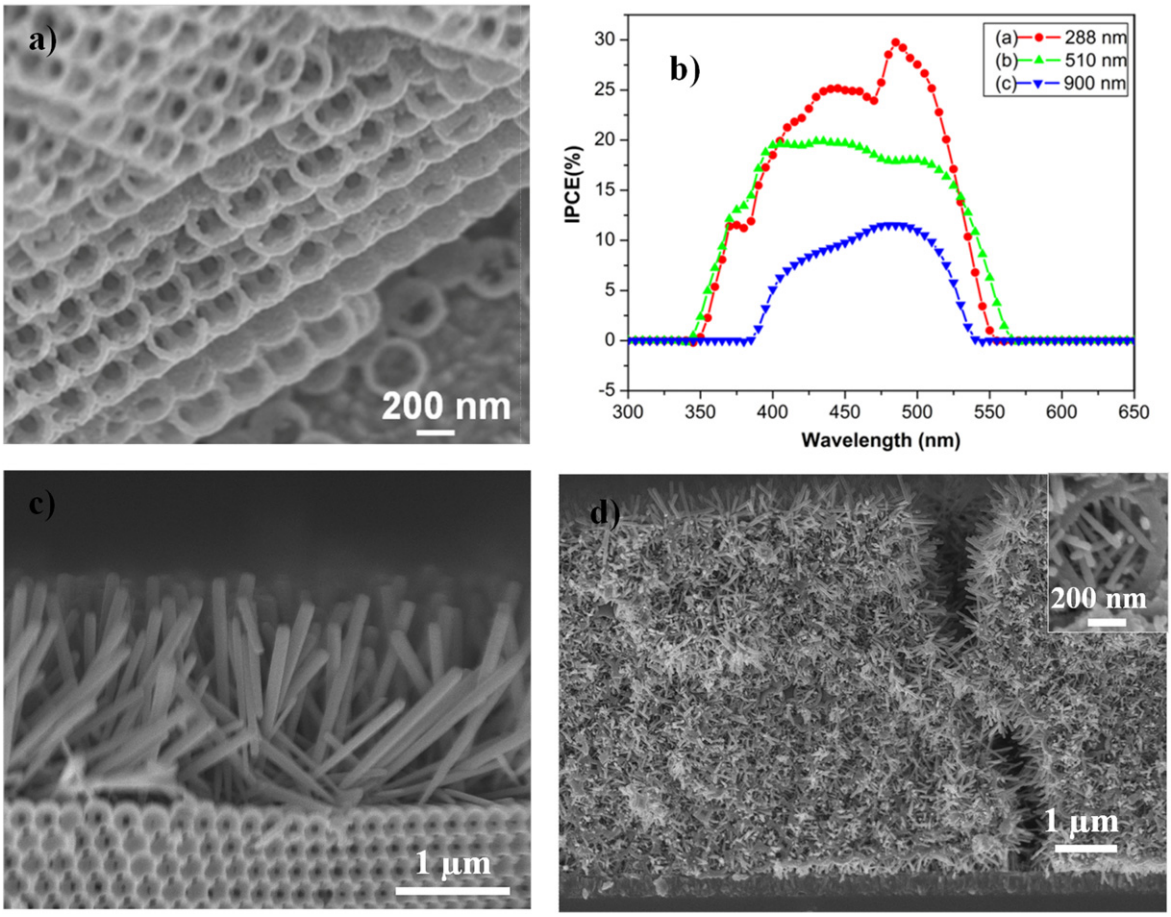

Figure 2. (a) FESEM image of CdS quantum dots sensitized TiO_2 inverse opal based on 288 nm polystyrene opals. (b) Incident photon to current conversion efficiency (IPCE) with TiO_2 inverse opal based photoanodes of different pore sizes. FESEM images of (c) ZnO nanowire arrays/TiO_2-inverse opal bilayer structure, (d) ZnO/TiO_2 nanobushes structure. Reprinted with permission from [21–23]. Copyright 2012 Wiley and Elsevier.

were fabricated using ALD based template replication of polystyrene opal templates, photosensitization of CdS quantum dots was achieved using SILAR method [20]. A promising photocurrent density of 4.84 mA cm^{-2} and an incident photon to current conversion efficiency (IPCE) maximum of ~30% have been attained for the 288 nm inverse opal as photoanode at 0 V versus Ag/AgCl bias under AM1.5 solar light illumination. The light harvesting efficiency of the TiO_2 inverse opal electrode could be further improved by forming a bilayer structure where ZnO nanowire arrays are grown directly on top of TiO_2 inverse opal. Upon TiO_2 infiltration of opal template by ALD, a ZnO seeding layer is deposited using ALD to allow the subsequent solution growth of ZnO nanowire arrays (figure 2(c)). Upon CdS sensitization, the bilayer electrode showed a photocurrent of ~5 mA cm^{-2} at 0.75 V versus Ag/AgCl, which is two times higher than that of the pure ZnO nanowire array electrode [21]. The improved photocurrent is ascribed to the photonic crystal serving as a 'dielectric mirror' that increased the optical path and improved light–matter interactions, thus enhancing the overall light harvesting efficiency. ALD was further employed to develop a 3D ordered hierarchical nanobushes, using TiO_2 inverse opal as a 3D host template for facile solution growth of networks of ZnO nanowires. In this work, TiO_2 inverse opals were coated with ~10 nm conformal ZnO film on TiO_2 shells using ALD and utilized as a 3D seed surface to grow the networks of ZnO nanowires using solution growth method and form nanobushes structure (figure 2(d)) [22]. The highest photocurrent density for nanobushes-CdS photoanode was observed to be 6.2 mA cm^{-2} at 0 V versus Ag/AgCl with an IPCE maximum of 60%, which is also the highest reported photocurrent density value for CdS/TiO_2 electrodes for PEC hydrogen generation.

2.2. Other types of electrodes

ALD has also been used to fabricate improved photocathode nanostructures for DSSCs via templated growth approach. It is possible to select an optimal template with desirable combination of nanostructure and physical properties for photocathodes without worrying about the chemical composition as ALD can be used to incorporate necessary material compositions. This approach was used to fabricate nanostructured electrodes for DSSCs from silica aerogel templates and depositing either ZnO or TiO_2 layers using ALD to impart the desired semiconducting properties (figure 3(a)) [24–26]. Similarly, anodic aluminum oxide

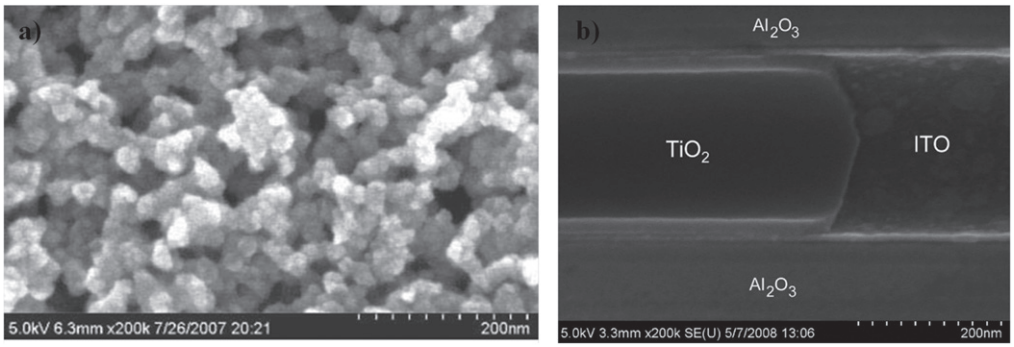

Figure 3. (a) SEM image of aerogel framework coated with 8.4 nm of ZnO. (b) Cross-sectional SEM image of a concentric TiO_2/ITO nanotube grown by ALD in AAO pores. Reprinted with permission from [24, 28]. Copyright 2008 Wiley and American Chemical Society.

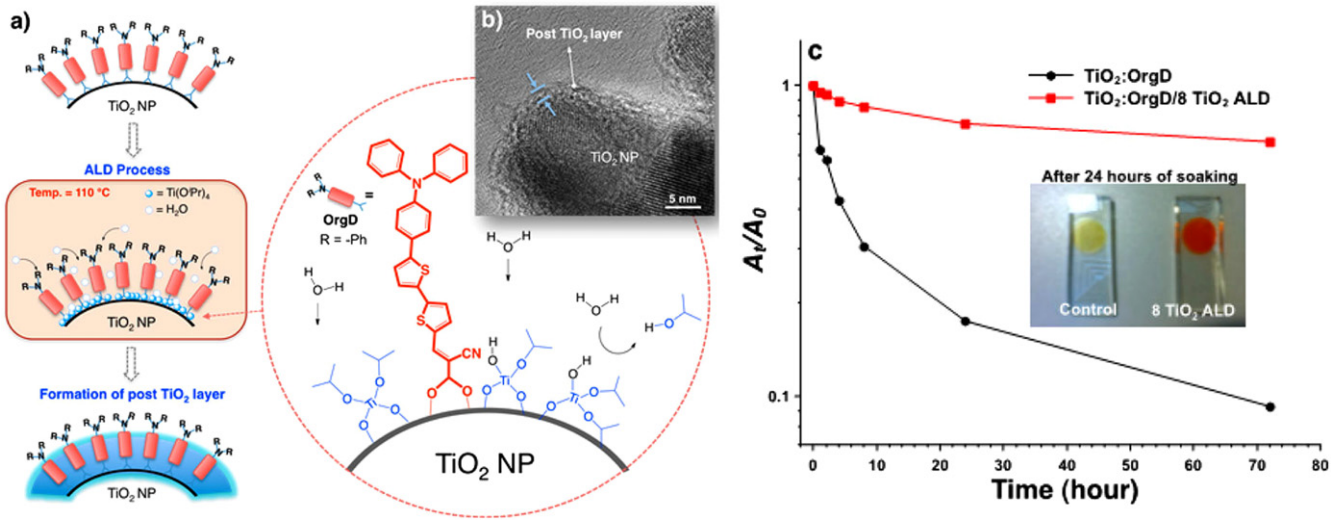

Figure 4. (a) Schematic illustration of the ALD TiO_2 layer on OrgD-sensitized solar cell photoanode surface with (b) the corresponding TEM image, and (c) the absorbance spectra of TiO_2/OrgD (black) and TiO_2/OrgD/ALD TiO_2 layer photoanodes as a function of soaking time in basic ethanol. Reprinted with permission from [33]. Copyright 2013 American Chemical Society.

(AAO) has been used to template ZnO-based DSSCs, which exhibited excellent photovoltages as a result of efficient charge transport through the 1D ZnO nanotubes [27]. The ease of fabrication and the flexibility of design make ALD based templated electrodes a promising candidate to advance DSSCs. In a conventional photoanode, photoelectrons need to diffuse through the entire thickness of the semiconducting photoanode before they are collected. During this diffusion process, electrons recombine with holes in the electrolyte resulting in energy losses. However, by depositing a transparent conducting material underneath the semiconducting layer, the electrons need only traverse the thicknesses of the order of few tens of nanometers to be collected. Using this technique, DSSCs were fabricated by depositing an ALD layer of TiO_2 onto transparent conducting indium tin oxide (ITO) [28, 29]. Figure 3(b) shows a cross-sectional SEM image of a single concentric TiO_2/ITO nanotube in 200 nm AAO pore. The underlying ITO was estimated to improve the photocurrent density by up to 60 times, clearly demonstrating the advantage of radial charge collection enabled by ALD.

3. Electrodes surface passivation via ALD

3.1. Surface passivation of photoanode in solar cells

For practical application of solar cells, long-term operation stability and high efficiency are highly required. Surface passivation could improve the photostability or viability of solar cells by isolating photoanode surface from surrounding environments, which is also in favor of the enhancement of efficiency by suppressing surface state recombination [12, 30, 31]. Initially, CVD technique was used to create surface passivation layer [32]. Compared with CVD, ALD provides a unique technique for the growth of passivation layer with excellent thickness and conformality control.

For DSSCs, its viability depends on the stability of surface-bound molecular chromophores. Detachment of molecular dyes from photoelectrode is one of the major limitations for the long-term operation stability. Recently, Son *et al* demonstrated the stabilization of small dye molecules on TiO_2 photoanode surfaces in OrgD-sensitized solar cells (OrgD = (E)-2-cyano-3-(5′-(5″-(p-(diphenylamino)phenyl)thiophen-2″-yl)thiophen-2′-yl)-acrylic acid) through post-

assembly ALD of additional TiO_2 layer (figure 4) [33]. The deposited TiO_2 layer covered anchoring-groups of OrgD molecules and protected them from water molecules and hydroxide ions, thus decreasing detachment from TiO_2 photoanode surface. In comparison with untreated film, ALD TiO_2 layer reduced desorption rate of dye molecules by more than 50 times [33]. When increasing the thickness of ALD TiO_2 overlayer, desorption rate exponentially decreases [31, 33]. Although increasing the deposited oxide layer increases the stability of solar cells, it reduces interface electron injection efficiency from sensitizer to the conduction band of photoanode oxide, due to either the increase of conduction band potential of TiO_2 and/or the weakening of electronic coupling between electrons in dye and TiO_2 [34–36], which would reduce the overall efficiency. Therefore, it is important to find a balance between them to optimize device performance. As the ALD deposited oxide layer isolated anchoring-groups from water molecules or hydroxide ions, this method has been used to improve the stability of various dye sensitizers (such as $[Ru(bpy)2(4,4'\text{-}(PO_3H_2)bpy)]^{2+}$, N719, N3 and Z907) in aqueous conditions [12, 33, 34, 37, 38], and various oxide passivation layer such as Al_2O_3 and Ga_2O_3 have also been ALD deposited [12, 33, 34, 37, 38].

In addition to improved stability, ALD treatment of DSSCs converts the initially dye-coated hydrophobic surface into a hydrophilic surface. The initial TiO_2/dye surface is usually hydrophobic due to the phenyl and/or alkyl terminating groups of adsorbed dyes. After ALD, TiO_2 or other oxide layers extend to near the dye termini, resulting in the hydrophilic TiO_2/dye/ALD layer surface, which is in favor of the permeation of aqueous electrolyte into photoelectrode mesopores, thus decreasing the limitation of photocurrent output due to constraining dye/aqueous solution and electrode/aqueous solution contact [31, 33].

Apart from DSSCs, ALD layer was also reported for the surface passivation of Si solar cells to reduce surface recombination and improve efficiency [39–41]. For example, Wang *et al* reported the improved efficiency of Si solar cells by suppressing surface recombination as well as reflection through ALD Al_2O_3 passivation layer [42]. The results revealed the improvement of short-circuit current density and efficiency by 8% and 10.3% respectively, realizing up to 18.2% conversion efficiency. In other works, the conversion efficiency as high as 23.2% was achieved in n-type Si solar cell with Al_2O_3 passivation layer [43–45], and surface recombination velocities below 10 cm s^{-1} was obtained in p-type Si solar cell [46]. Similarly, ALD application in emergent perovskite solar cells for the growth of a highly compact TiO_2 layer for efficient hole-blocking has also been demonstrated [47].

3.2. Surface passivation of photoabsorber for solar water splitting

As PEC cell is based on a semiconductor/liquid junction, the semiconductor photoelectrodes must be stable in aqueous environments. However, many of the semiconductors used for PEC water splitting, such as Si, Cu_2O, InP, ZnO, are not stable at the highly oxidative potentials required for water oxidation [48–52]. Fortunately, the stability of these semiconductors can be improved with a thin protectively insulative layer. The thickness of the protective layer should be very thin, for example several tens nanometers, otherwise the charge transfer between the semiconductor and liquid will be blocked. In addition, to function as a protective layer, it should be very dense and have excellent conformality. Among various thin film deposition methods, only ALD can meet these demands. Indeed, the ALD TiO_2 thin films have been used to improve the stability of photoelectrodes of solar water splitting. For example, Thimsen *et al* demonstrated that the photocurrent of electrodeposited Cu_2O photocathode only drops to 78% to the initial photocurrent with 11 nm ALD TiO_2 as protective layer after 20 min, while without ALD TiO_2 protective layer it shows no photocurrent at all [50]. It has also been reported that the ALD TiO_2 can be used as a corrosion-resistant layer to protect the Si based photoanode without inhibiting charge carrier (electron or hole) transport and photon absorption. The sample with the corrosion resistant ALD TiO_2 (2 nm) layer remained operational for at least 24 h, whereas the sample without the TiO_2 layer failed within 0.5 h [51]. Jeol *et al* reported that the ALD TiO_2 can be used as protective layer to improve the stability of InP nanopillar photocathodes [52]. Very recently, Hu *et al* reported ALD TiO_2 films (4–143 nm thick) to protect Si, as well as GaAs and GaP photoanodes for efficient water oxidation from photocorrosion [49]. For example, in conjunction with Ni oxide electrocatalysts, ALD TiO_2–Si photoanodes exhibited continuous oxidation for more than 100 h at photocurrent densities of >30 mA cm^{-2} in 1.0 M KOH solution. And ALD TiO_2-protected GaAs and GaP photoelectrodes exhibited photovoltages of 0.81 and 0.59 V, and photocurrent densities of 14.3 and 3.4 mA cm^{-2}, respectively [49]. Meyer and coworkers reported the enhanced surface binding stability of a phosphonate-derivatized water oxidation catalyst over a wide pH range (1–12) by ALD TiO_2 [53]. Increased stabilization of surface binding allows use of basic solutions where a rate enhancement for water oxidation of $\sim 10^6$ is observed compared with acidic conditions. These experiments suggest that the stability of photoelectrodes can be significantly enhanced by an ALD thin film, which may be suitable for long-term PEC applications.

Among various photo-absorber materials for PEC, hematite (α-Fe_2O_3) is one promising photoanode material due to its favorable optical band gap (~2.1 eV), chemical stability in aqueous environments, elemental abundance and low cost [54, 55]. However, the overall water splitting efficiency of hematite photoanodes is still lower than the theoretically maximum efficiency, which is primarily attributed to short hole diffusion length (~10 nm) compared to the light penetration depth of several hundred nanometers [56]. One possibility to overcome the drawback is to have non-conventional photoelectrode design, i.e. nanorods or nanowires, which is characterized by both short charge-collection distances and high surface areas. However, the surface traps at the surface of nanostructured

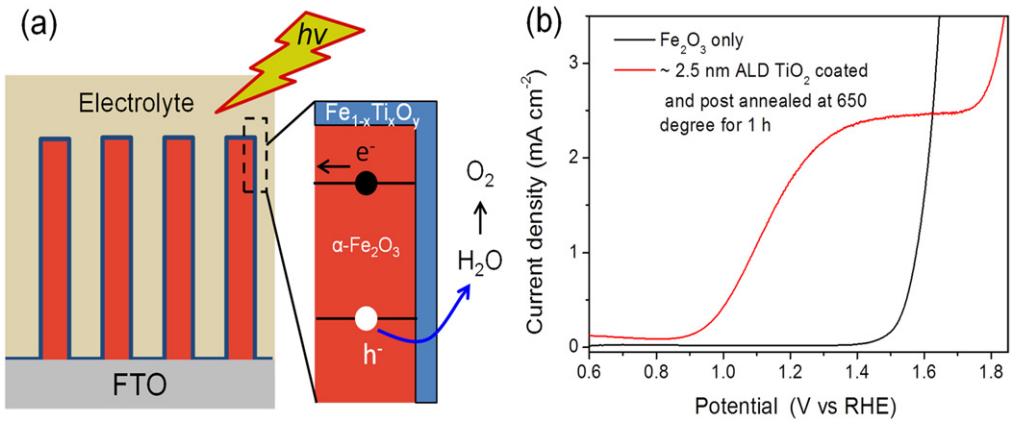

Figure 5. (a) Schematic of the hematite nanorods array coated with an ultrathin $Fe_xTi_{1-x}O_y$ layer for efficient water oxidation (b) Photocurrent–potential (*J–V*) curves for PEC water oxidation reaction hematite nanorod arrays photoanodes with and without the $Fe_xTi_{1-x}O_y$ layer.

water splitting hematite photoanodes may reduce the efficiency due to an increase in charge recombination rate at the surface [57]. Despite the nanostructuring efforts, a second crucial drawback of hematite remains: an additional high over potential (0.5–0.6 V) required to initiate water oxidation represents a significant energy loss [58]. Attaching co-catalyst materials on the nanostructured hematite photoanodes can lower the over potential [59, 60]. The passivation of the surface states and catalyst loading require a good technique to provide uniform coating on nanostructured hematite photoanodes. For this purpose, ALD stands out to be the most suitable method due to its capability of conformal coating on arbitrary-shape surfaces and atomic level control in film thickness. For example, a 100 mV photocurrent onset cathodic shift was observed on cauliflower-like silicon-doped hematite grown by atmospheric pressure chemical vapor deposition, through a very thin ALD Al_2O_3 (0.1–2 nm) coating [58]. The cathodic shift afforded by the Al_2O_3 overlayer is due to the passivation of surface states. Martinson and their co-workers reported that the ALD-coated sub monolayer catalysts using $Co(Cp)_2$ and O_3 as precursors on hematite photoanode results in a significant decrease in the applied potential required to drive water oxidation [58].

Recently, Li *et al* have found that an ultrathin amorphous $Fe_xTi_{1-x}O_y$ layer on the hematite nanorod surface results in significant increase of the photocurrent density, which can go up to 1.9 mA cm^{-2} at 1.23 V versus RHE in 1 M NaOH solution, while the reference sample without $Fe_xTi_{1-x}O_y$ layer shows negligible photocurrent (figure 5). The ultrathin amorphous $Fe_xTi_{1-x}O_y$ layer was obtained by annealing the ALD TiO_2 coated hematite sample at 650 °C. The amorphous $Fe_xTi_{1-x}O_y$ layer thickness plays an important role to the overall photocurrent. If the amorphous $Fe_xTi_{1-x}O_y$ layer is too thin, it cannot provide sufficient passivation of the surface states. While it is too thick, the hole transfer from hematite to liquid will be blocked. The optimized passivation layer was obtained from ALD TiO_2 thickness ~2.5 nm (40 ALD cycles) and 1 h post annealing at 650 °C.

4. Surface sensitization

4.1. Quantum dots sensitization

Surface sensitization is a fundamental and important approach to improve light harvesting and conversion efficiency of solar energy in various light-harvesting devices. Quantum dots sensitization provides potential for the design of next generation solar cells as their high theoretical conversion efficiency. Conventional methods for depositing quantum dots photosensitizers such as dip coating, electrochemical deposition and CVD suffer from poor control in thickness and uniformity. By employing ALD for quantum dots sensitization, excellent infiltration and conformity could be achieved, and the size of quantum dots can be controlled simply by tuning the number of ALD cycles. For example, Brennan *et al* realized ALD CdS quantum dots sensitized solid-state solar cells, using dimethyl cadmium and *in situ* generated H_2S as cadmium and sulfur precursors respectively [61]. Results showed the performance of solar cells was dependent on the number of ALD cycles, and the maximum photocurrent was obtained in five ALD cycles. Further increasing ALD cycles resulted in the decrease of cell efficiency. This is may be due to the overgrowth of CdS increased the aggregation of nanoparticles, which increases the recombination sites and decreases the filling efficiency of hole-conductor [61].

PbS, as narrow bandgap quantum dots, was also reported via ALD in the sensitization of Si solar cell using bis(2,2,6,6-tetramethyl-3,5-heptanedionato)lead(II) and H_2S as precursors [62]. The deposited PbS was uniformly coated onto the surface of Si wires in the form of isolated nanoparticles. The size varied from 5 to 25 nm with increasing the number of ALD cycles from 10 to 80 as shown in figure 6. It is indicated that ALD is a unique and powerful tool to conformally coat a single layer of QDs with controlled size. Other sulfides sensitizer such as In_2S_3 was also deposited for solar energy conversion [63]. During processing of In_2S_3, ALD displayed a nucleation period of 60–70 cycles on initial surfaces, and the growth per cycle decreased from 0.28 Å 130 °C to 0.15 Å per cycle at 170 °C due to the incomplete self-

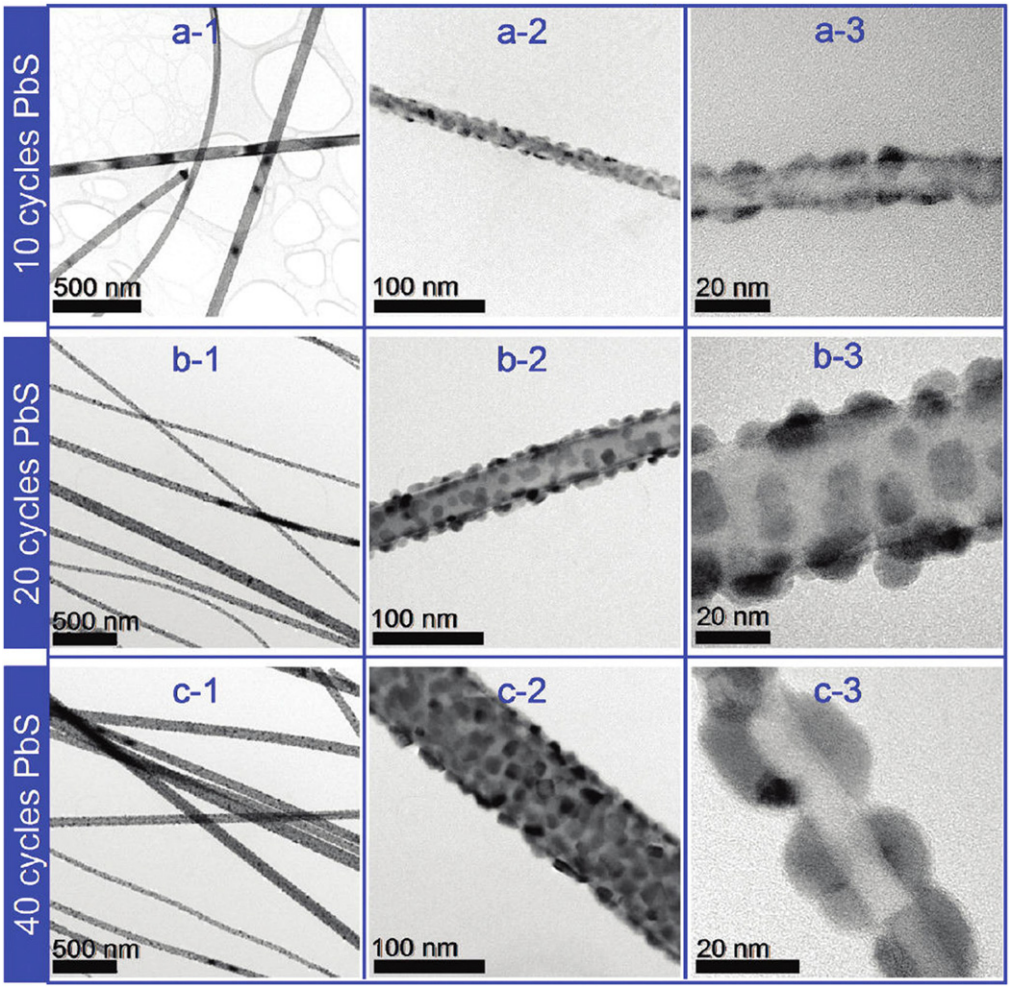

Figure 6. TEM images of ALD technique deposited PbS on Si nanowires for (a) 10 cycles, (b) 20 cycles, and (c) 40 cycles ethanol. Reprinted with permission from [62]. Copyright 2011 American Chemical Society.

limiting $In(acac)_3$ reaction. Though many papers have reported ALD sulfides as sensitizer for solar energy conversion, we note that all those sensitizers were deposited using H_2S as sulfur precursor. It is known H_2S is a highly toxic and corrosive gas, which expose users to huge safety risk when use it. Thus, developing safe and eco-friendly sulfur precursors is highly required.

Alternatively, ALD also provides an indirect approach for the sensitization of quantum dots etc. Luo and Karuturi *et al* demonstrated CdSe quantum dots photosensitization method by ALD depositing sacrificial ZnO thin films on various TiO_2 nanostructures, anion solution exchange of ZnO layer to ZnSe, and finally cation solution exchange of intermediate ZnSe to CdSe. PEC performance tests to CdSe-sensitized TiO_2 inverse opal photoanodes revealed a drastically improved photocurrent level, up to 15.7 mA cm^{-2} at zero bias (versus Ag/AgCl), more than double that by conventional techniques such as SILAR (figure 7) [64]. Moreover, ALD was applied as an effective technique to integrate the up-conversion nanomaterials in photoeletrodes for efficient solar energy conversion by broadening the spectral photoresponse. A heteronanostructured photoanode was developed by encapsulating up-conversion nanoparticles with electron transporting TiO_2 using ALD. The resultant hetero-nanostructure was sensitized with CdSe quantum dots and demonstrated for near-infrared PEC hydrogen generation through an *in situ* photon up-conversion of near-infrared light to visible wavelengths [65].

4.2. Metal nanoparticles sensitization

Similarly, ALD metal nanoparticles sensitization provides a promising approach to improve the conversion of solar energy by catalysis in PEC water splitting. Dasgupta *et al* revealed that Si nanowire arrays with ALD sensitized Pt nanoparticles exhibited the current densities from 7 to 21 mA cm^{-2} at 0 V versus RHE (AM 1.5) with increasing the number of ALD cycles from 1 to 10 [66], while there was no photo-activity with Si alone, indicating the tunability of catalytic activity of Pt nanoparticles by varying the number of ALD cycles. And an onset voltage of 0.15–0.25 V versus RHE and current densities of ~30 mA cm^{-2} were shown for all photoanodes [66]. All samples exhibited comparable PEC performance to previous reported standard Pt sensitization technique. Importantly, the corresponding surface loadings of ALD Pt nanoparticles were as low as 13–105 ng cm^{-2}, it is indicated

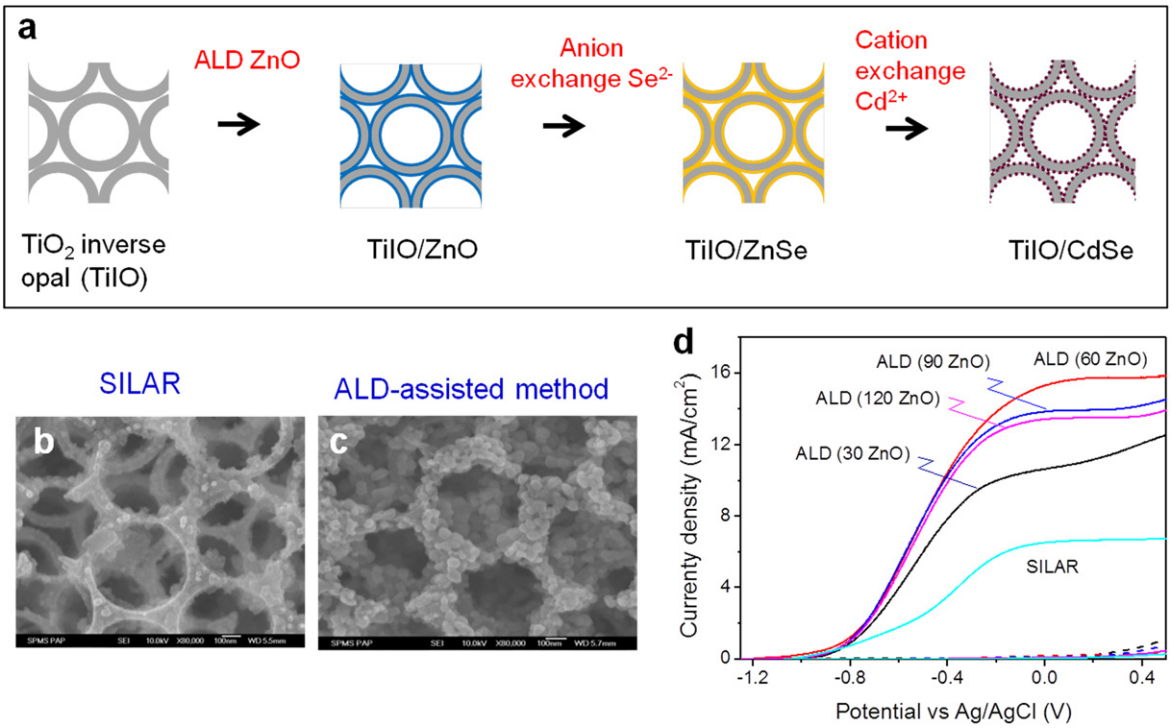

Figure 7. A new method for the fabrication of chalcogenide semiconductor photosensitizers enabled by ALD. (a) Fabrication process based on TiO_2 inverse opal photoanode. (b) SEM image of the TiO_2 inverse opal sensitized by CdSe particles using conventional SILAR method. (c) SEM image of the TiO_2 inverse opal sensitized by CdSe particles using ALD-assisted method. (d) Photocurrent versus potential for the TiO_2 inverse opal PEC anode. Reprinted with permission from [64]. Copyright 2012 Nature publishing.

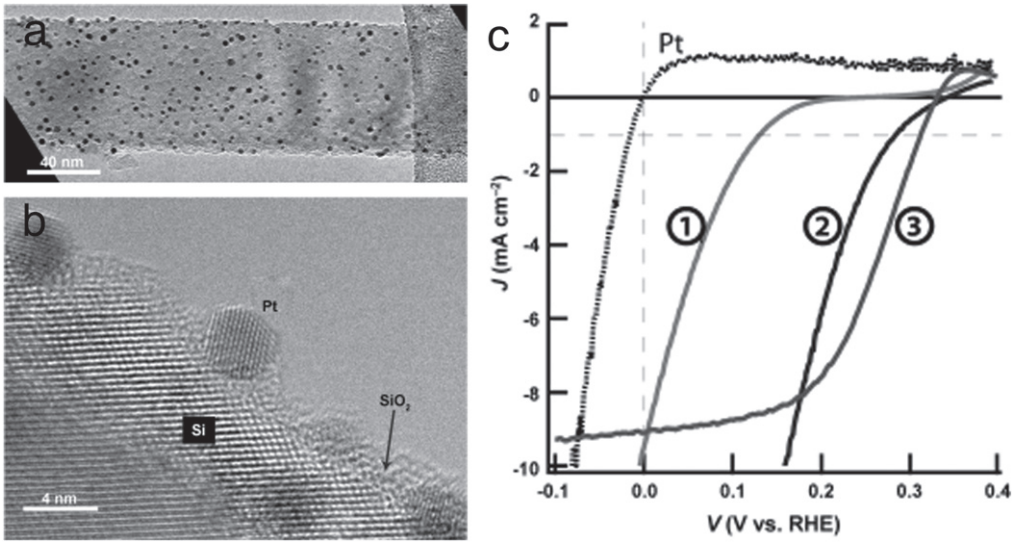

Figure 8. (a) TEM and (b) HRTEM images of Pt nanoparticles deposited on Si nanowire by ALD Pt, and (c) polarization curves of various eletrodes in hydrogen evolution reaction environments. 1, 2 and 3 represent bare Si nanowires, Si nanowires with electroless-deposited Pt, and Si nanowires with ALD Pt, respectively. Reprinted permission from [67]. Copyright 2013 Wiley.

that ALD is an effective tool for the ultralow loading of Pt nanoparticles without reducing catalytic performance, thus potentially reducing the use costs of noble-metal catalysts.

In addition, Pt nanoparticles catalyst deposited by other techniques predominantly reside on the tips of Si nanowire arrays, which increases the diffusion distance for the collection of electrons (figure 8) [67]. On the contrary, ALD deposited Pt nanoparticles uniformly covered on the surface of Si nanowire arrays, achieving the efficient collection of photogenerated charges, thus improving PEC water splitting efficiency. Analogously, this technique could easily be extended to the preparation of metal-plasmon enhanced solar cells, however, the relevant information is rarely reported up till now.

5. Band-structure engineering via ALD

5.1. Band-structure engineering in DSSCs

Much effort has been put into band gap engineering in DSSCs so as to improve the conversion efficiencies of the cells. Conventionally, wide band gap semiconductors nanoparticles are being used as the photoanode material due to their inherent high surface area [68]. Recent developments to enhance the absorption capability of the photoanode include employing 3D hierarchical nanostructures such as inverse opals in place of conventional TiO_2 nanoparticles [69]. However, the adsorption band gap needs to be tuned in order to achieve higher conversion efficiencies. The adsorption band gap is determined by the inherent property of the photosensitizer. Conventional photosensitizers that are used are based on Ru complexes, which typically have conversion efficiencies over 10% and absorption of around over 500 nm [70]. However, due to the high cost of ruthenium, alternative photosensitizers such as metal free dyes are currently being explored.

Although the adsorption band gap is determined by the material type, the efficiency of the electrode is limited by carrier recombination that happens with the electrolyte. To address that issue, ALD is being employed to reduce these recombination processes. With ALD, a thin and conformal coating of a high band gap metal oxide between the photosensitive layer and the substrate can be achieved. However, with barrier layers like Al_2O_3, HfO_2, the electron transfer efficiency to the substrate (e.g. TiO_2) sometimes decreases due to the fact that the conduction band of the barrier layer is usually higher than that of the substrate. However for some other metal oxides like Ta_2O_5 actually improved the electron transfer efficiency. As can be seen, there is considerable potential for ALD to be employed in optimizing the charge transfer efficiency by facilitating the carrier transport between the photosensitizers and substrate with varying band structures.

5.2. Buffer layer engineering in CIGS solar cell

Buffer layer is indispensable to the chalcopyrite-type thin-film solar cells based on CIGS and related absorbers such as $CuInS_2$, $Cu(In,Ga)(S,Se)_2$ and CuZnSnS, as it efficient charge separation and charge transport between the absorber and the ZnO window layer. The absence of such a buffer layer will result in a drop of open circuit voltage (V_{oc}) and poor efficiency, among others, due to the large negative conduction band offset (CBO, ΔE_c) at the CIGS/ZnO interface [71]. As there are intrinsic material limitations and industrial processing drawbacks of the commonly used CdS buffer layer, to find a substitute for CdS is one of the major objectives in the field of CIGS technology.

ALD provides thin films with excellent conformality and thickness control down to atomic level, which is capable to deposit a wide variety of Cd-free materials as a buffer layer in CIGS solar cells. As the growth rate per cycle of ALD is in the atomic level, excellent composition control over the film

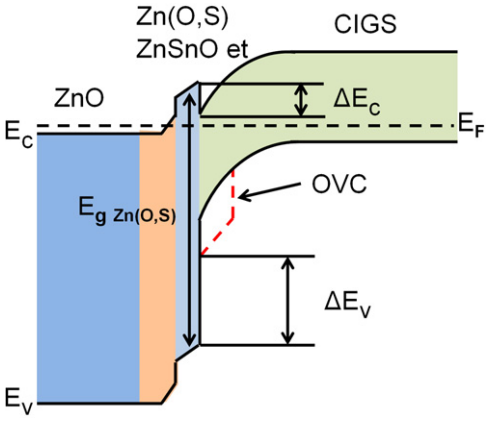

Figure 9. Band diagram of a CIGS thin-film solar cell with Cd-free buffer layers.

can be easily achieved through control of the precursor pulse ratios during the co-deposition process. Thus excellent control of the band gap and CBO can be achieved (figure 9). Moreover, ALD is a gas phase process that can be easily integrated alongside other vacuum processes. ALD Cd-free buffer layers have been extensively reviewed previously [4, 72, 73]. Zn(O,S), $Zn_{1-x}Sn_xO$, (Zn,Mg)O and In_2S_3 have been identified as the most promising Cd-free buffer layers for CIGS solar cells.

ALD Zn(O,S) buffer can be deposited by changing the ZnO and ZnS cycles using diethyl zinc (DEZ), $Zn(C_2H_5)_2$, precursor and H_2O and H_2S as reactants. The performance of the solar cell using ALD Zn(O,S) as buffer layer depends strongly on the S/(S + O) ratio of the buffer layer, which is controlled by the pulse ratios of H_2S/H_2O during the ALD process. On the one hand, when S/(S + O) ratio is too high, an ultrathin buffer layer is required to prevent charge recombination in this layer. On the other hand, the Voc of the solar cell drops if the S/(S + O) ratio is too low. Both phenomena can be explained by the ΔE_c at the CIGS/Zn(O,S) interface, which has been intensively discussed by Plater-Björkman *et al* [74–77]. ΔE_c ranging from 0 to 0.4 eV was calculated to be well suited to reach high performance (figure 10). Over 18.0% efficiency of CIGS solar cells with ALD Zn(O,S) buffer layers was reported by many groups. The absorption of these cells with Zn(O,S) buffer layers in the short wavelength range is much better than that of the reference cell using CdS as buffer layers, resulting in an increased J_{sc} and efficiency.

$Zn_{1-x}Sn_xO$ is a new alternative buffer layer for CIGS solar cells, which also benefit from the ability of ALD to control the film composition from pure ZnO to pure SnO_x by changing the ratio between the DEZ and TDMASn, $Sn(N(CH_3)_2)_4$, precursors and the H_2O reactant [78, 79]. Similar to Zn(O,S), the band gap and the CBO can be controlled by the Sn/(Sn + Zn) ratio of the $Zn_{1-x}Sn_xO$ buffer layer. However, the difference is that the ALD $Zn_{1-x}Sn_xO$ buffer layers are amorphous, which is an interesting property because it reduces the amount of recombination centers at the grain boundaries in the bulk buffer layer and at the CIGS/buffer interface. The best $Zn_{1-x}Sn_xO$ buffer layer had an Sn/(Sn + Zn) ration between 15% and 20% deposited at 120 °C. The

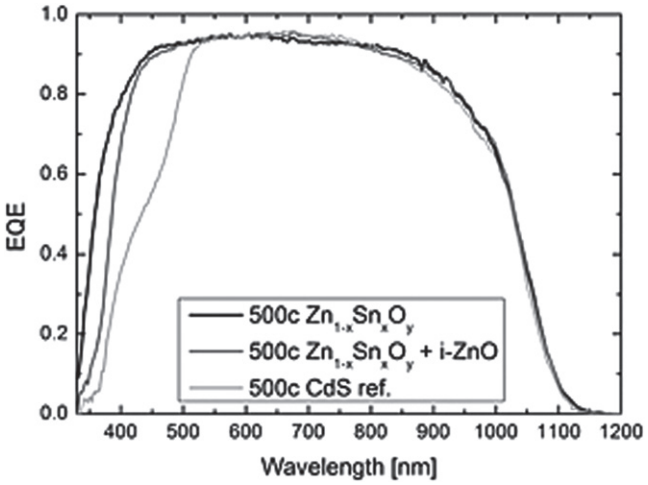

Figure 10. Average external quantum efficiency curves from five cells from the ALD $Zn_{1-x}Sn_xO$, $Zn_{1-x}Sn_xO$ + i-ZnO and CdS ref samples. Reprinted permission from [78]. Copyright 2013 Wiley.

application of these 25 nm thick $Zn_{1-x}Sn_xO$ buffer layers on coevaporated CIGS solar cell led to efficiencies up to 18.0%, which is comparable to that with CdS buffer layer [78]. The higher J_{sc} obtained for the $Zn_{1-x}Sn_xO$ compared with CdS reference samples are expected, as the band gap of the CdS is lower than that of $Zn_{1-x}Sn_xO$ (3.0 eV) (figure 10) [78, 80]. Due to the Voc drop of the cell with $Zn_{1-x}Sn_xO$ buffer layers, the overall efficiency is not better than the CdS reference cell.

ALD (Zn,Mg)O buffer layers are usually deposited by alternating ZnO and MgO cycles using $Zn(C_2H_5)_2$, $MgCp_2$ as precursors and H_2O as reactant. By tuning the Mg/(Zn + Mg) ratio, the band gap of the as deposited (Zn,Mg)O buffer layers can be controlled from 3.3 eV to 3.8 eV [71, 81]. The optimized (Zn,Mg)O buffer layers with a band gap of about 3.6 eV were deposited at 120 °C. Due to the lower Voc and fill factor values, a significant drop in cell efficiency was observed with (Zn,Mg)O buffer layers deposited at higher temperatures, which could be due to the deterioration of the interface quality. The co-evaporated CIGS cells with ALD (Zn,Mg)O buffer layer (150 nm thick) yielded efficiencies up to 18.1% [82].

ALD-In_2S_3 buffer layers can be deposited using $In(acac)_3$ and H_2S as precursors. The deposition temperature is relatively higher compared to that of (Zn,Mg)O and Zn(O,S), typically 200–210 °C. It has been reported that the interface diffusion happens between the CIGS absorber and In_2S_3 layer during the deposition process at such a high temperature [83]. If Cu is present in excess in the In_2S_3 buffer layer, the p–n junction formed between CIGS and In_2S_3 may be deteriorated. At the same time, the occupation of Cu vacancies by In ions will imply the inversion of the near-interface region of CIGS from p-type to n-type and form a buried junction in the CIGS layer [83]. The highest cell efficiencies up to 16.4% have been reported for cells with ALD In_2S_3 buffer layers of 30–40 nm [84, 85]. As the band gap of In_2S_3 (2.7 eV) is larger than CdS (2.4 eV), the quantum efficiency of the devices with In_2S_3 buffer layers is higher than the CdS reference device in the short wavelength range. Compared to other alternative Cd-free buffer layers, the main advantage for In_2S_3 buffer layers is that the cell does not suffer from the light soaking effect [86].

6. Conclusions

We have summarized and discussed the emergent application of ALD in solar cell research, including the fabrication of PEC photoanodes, sensitization of TiO_2 nanostructured PEC anode by semiconductor nanoparticles and Si nanowire photocathode by highly dispersed noble metal nanoparticles, and surface passivation of Si and CIGS thin film solar cells. Most solar devices materials have stability issues, either due to photocorrosion, etching, or simply dissolution into electrolyte, and thus hurdle the practical application of these high-potential materials. A uniform coated atomic thin film rendered by ALD could address this problem via various mechanisms. In the particular case of thin film solar cells and PEC cells, an ALD film in some circumstances is not simply a 'passivation' but constructs a thin heterojunction interface; the resulting built-in potential is beneficial to the photo charge separation. In addition, doping is highly desirable for all solar applications but this has been a challenge. Some success has been achieved mainly for Al/Ga/Ti-doped ZnO and Ta-doped TiO_2 and more intensive research is needed for materials like Fe_2O_3 and WO_3. Of particular interest is the ALD metal which naturally form well dispersed nanoparticles rather than thin films. This will be extremely useful for photocatalyst or electrocatalyst. In short, with the increasing interest in energy and environment related research, ALD will continue to play an increasingly important role and most likely become a mainstream facility.

Acknowledgments

H J Fan acknowledges the financial support by MOE AcRF Tier 1 (RG 66/11), and SERC Public Sector Research Funding (Grant number 1121202012), Agency for Science, Technology, and Research (A*STAR), Singapore. The authors also acknowledge support from the Energy Research Institute @NTU (ERI@N). We also acknowledge the reuse permission from Royal Chemical Society. X Li and L H Wong acknowledge funding from NRF Energy Innovation Programme Office (NRF2001EWT-CERP001-019).

References

[1] Pinna N and Knez M 2012 *Atomic Layer Deposition of Nanostructured Materials* 1st edn (Weinheim: Wiley-VCH)
[2] Detavernier C, Dendooven J, Pulinthanathu Sree S, Ludwig K F and Martens J A 2011 Tailoring nanoporous materials by atomic layer deposition *Chem. Soc. Rev.* **40** 5242–53
[3] Marichy C, Bechelany M and Pinna N 2012 Atomic layer deposition of nanostructured materials for energy and environmental applications *Adv. Mater.* **24** 1017–32

[4] Bakke J R, Pickrahn K L, Brennan T P and Bent S F 2011 Nanoengineering and interfacial engineering of photovoltaics by atomic layer deposition *Nanoscale* **3** 3482–508

[5] Meng X, Yang X Q and Sun X 2012 Emerging applications of atomic layer deposition for lithium-ion battery studies *Adv. Mater.* **24** 3589–615

[6] Liu M, Li X, Karuturi S K, Tok A I Y and Fan H J 2012 Atomic layer deposition for nanofabrication and interface engineering *Nanoscale* **4** 1522–8

[7] Guan C, Xia X, Meng N, Zeng Z, Cao X, Soci C, Zhang H and Fan H J 2012 Hollow core–shell nanostructure supercapacitor electrodes: gap matters *Energy Environ. Sci.* **5** 9085–90

[8] Jung Y S, Cavanagh A S, Dillon A C, Groner M D, George S M and Lee S H 2010 Enhanced stability of $LiCoO_2$ cathodes in lithium-ion batteries using surface modification by atomic layer deposition *J. Electrochem. Soc.* **157** A75–81

[9] Lu J, Lei Y and Elam J W 2012 Atomic layer deposition of noble metals—new developments in nanostructured catalysts (Rijeka: InTech)

[10] Liu L, Karuturi S K, Su L T, Wang Q and Tok A I Y 2011 Electrochromic photonic crystal displays with versatile color tunability *Electrochem. Commun.* **13** 1163–5

[11] Mihi A, Calvos M E, Anta J A and Míguez H 2008 Spectral response of opal-based dye-sensitized solar cells *J. Phys. Chem.* C **112** 13–7

[12] Tetreault N, Arsenault E, Heiniger L P, Soheilnia N, Brillet J, Moehl T, Zakeeruddin S, Ozin G A and Gratzel M 2011 High-efficiency dye-sensitized solar cell with three-dimensional photoanode *Nano Lett.* **11** 4579–84

[13] Nishimura S, Abrams N, Lewis B A, Halaoui L I, Mallouk T E, Benkstein K D, Van de Lagemaat J and Frank A J 2003 Standing wave enhancement of red absorbance and photocurrent in dye-sensitized titanium dioxide photoelectrodes coupled to photonic crystals *J. Am. Chem. Soc.* **125** 6306–10

[14] Mihi A and MÃ-guez H 2005 Origin of light-harvesting enhancement in colloidal-photonic-crystal-based dye-sensitized solar cells *J. Phys. Chem.* B **109** 15968–76

[15] Mihi A, Calvos M E, Anta J A and MÃ-guez H 2008 Spectral response of opal-based dye-sensitized solar cells *J. Phys. Chem.* C **112** 13–7

[16] Karuturi S K, Liu L, Su L T, Zhao Y, Fan H J, Ge X, He S and Tok A I Y 2010 Kinetics of stop-flow atomic layer deposition for high aspect ratio template filling through photonic band gap measurements *J. Phys. Chem.* C **114** 14843–8

[17] Liu L, Karuturi S K, Su L T and Tok A I Y 2011 TiO_2 inverse-opal electrode fabricated by atomic layer deposition for dye-sensitized solar cell applications *Energy Environ. Sci.* **4** 209–15

[18] Fujishima A and Honda K 1972 Electrochemical photolysis of water at a semiconductor electrode *Nature* **238** 37–41

[19] Kamat P V, Tvrdy K, Baker D R and Radich J G 2009 Beyond photovoltaics: semiconductor nanoarchitectures for liquid-junction solar cells *Chem. Rev.* **110** 6664–88

[20] Alibabaei L, Brennaman M K, Norris M R, Kalanyan B, Song W J, Losego M D, Concepcion J J, Binstead R A, Parsons G N and Meyer T J 2013 Solar water splitting in a molecular photoelectrochemical cell *Proc. Natl. Acad. Sci. USA* **110** 20008–13

[21] Cheng C, Karuturi S K, Liu L, Liu J, Li H, Su L T, Tok A I Y and Fan H J 2012 Quantum-dot-sensitized TiO_2 inverse opals for photoelectrochemical hydrogen generation *Small* **8** 37–42

[22] Karuturi S K, Cheng C, Liu L, Su T L, Fan H J and Tok A I Y 2012 Inverse opals coupled with nanowires as photoelectrochemical anode *Nano Energy* **1** 322–7

[23] Karuturi S K, Luo J, Cheng C, Liu L, Su L T, Tok A I Y and Fan H J 2012 A novel photoanode with three-dimensionally, hierarchically ordered nanobushes for highly efficient photoelectrochemical cells *Adv. Mater.* **24** 4157–62

[24] Hamann T W, Martinson A B F, Elam J W, Pellin M J and Hupp J T 2008 Aerogel templated ZnO dye-sensitized solar cells *Adv. Mater.* **20** 1560–4

[25] Hamann T W, Martinson A B F, Elam J W, Pellin M J and Hupp J T 2008 Atomic layer deposition of TiO_2 on aerogel templates: new photoanodes for dye-sensitized solar cells *J. Phys. Chem.* C **112** 10303–7

[26] Chandiran A K, Yella A, Stefik M, Heiniger L P, Comte P, Nazeeruddin M K and Gratzel M 2013 Low-Temperature crystalline titanium dioxide by atomic layer deposition for dye-sensitized solar cells *ACS Appl. Mater. Interfaces* **5** 3487–93

[27] Martinson A B F, Elam J W, Hupp J T and Pellin M J 2007 ZnO nanotube based dye-sensitized solar cells *Nano Lett.* **7** 2183–7

[28] Martinson A B F, Elam J W, Liu J, Pellin M J, Marks T J and Hupp J T 2008 Radial electron collection in dye-sensitized solar cells *Nano Lett.* **8** 2862–6

[29] Alibabaei L, Farnum B H, Kalanyan B, Brennaman M K, Losego M D, Parsons G N and Meyer T J 2014 Atomic layer deposition of TiO_2 on mesoporous nanoITO: conductive core–shell photoanodes for dye-sensitized solar cells *Nano Lett.* **14** 3255–61

[30] Pascoe A R, Bourgeois L, Duffy N W, Xiang W C and Cheng Y B 2013 Surface state recombination and passivation in Nanocrystalline TiO_2 dye-sensitized solar cells *J. Phys. Chem.* C **117** 25118–26

[31] Hanson K, Losego M D, Kalanyan B, Parsons G N and Meyer T J 2013 Stabilizing small molecules on metal oxide surfaces using atomic layer deposition *Nano Lett.* **13** 4802–9

[32] Hezel R and Jaeger K 1989 Low-temperature surface passivation of silicon for solar-cells *J. Electrochem. Soc.* **136** 518–23

[33] Son H J, Prasittichai C, Mondloch J E, Luo L L, Wu J S, Kim D W, Farha O K and Hupp J T 2013 Dye stabilization and enhanced photoelectrode wettability in water-based dye-sensitized solar cells through post-assembly atomic layer deposition of TiO_2 *J. Am. Chem. Soc.* **135** 11529–32

[34] Hanson K, Losego M D, Kalanyan B, Ashford D L, Parsons G N and Meyer T J 2013 Stabilization of [Ru(bpy)(2)(4,4′-(PO_3H_2)bpy)]$^{(2+)}$ on mesoporous TiO_2 with atomic layer deposition of Al_2O_3 *Chem. Mater.* **25** 3–5

[35] Antila L J, Heikkila M J, Aumanen V, Kemell M, Myllyperkio P, Leskela M and Korppi-Tommola J E I 2010 Suppression of forward electron injection from Ru(dcbpy)(2)(NCS)(2) to nanocrystalline TiO_2 film as a result of an interfacial Al_2O_3 barrier kayer prepared with atomic layer deposition *J. Phys. Chem. Lett.* **1** 536–9

[36] Antila L J *et al* 2011 ALD grown aluminum oxide submonolayers in dye-sensitized solar cells: the effect on interfacial electron transfer and performance *J. Phys. Chem.* C **115** 16720–9

[37] Hamann T W, Farha O K and Hupp J T 2008 Outer-sphere redox couples as shuttles in dye-sensitized solar cells. performance enhancement based on photoelectrode modification via atomic layer deposition *J. Phys. Chem.* C **112** 19756–64

[38] Chandiran A K, Tetreault N, Humphry-Baker R, Kessler F, Baranoff E, Yi C Y, Nazeeruddin M K and Gratzel M 2012 Subnanometer Ga_2O_3 tunnelling layer by atomic layer feposition to achieve 1.1 V open-circuit potential in dye-sensitized solar cells *Nano Lett.* **12** 3941–7

[39] Jeong K S, Kwon H M, Lee H D and Lee G W 2014 Ultra-thin aluminum oxide as an interface passivation layer for ZnO/p-Si heterojunction solar cells *Phys. Status Solidi* A—*Appl. Mater. Sci.* **211** 1850–6

[40] Jeong K S, Oh S K, Shin H S, Yun H J, Kim S H, Lee H R, Han K M, Park H Y, Lee H D and Lee G W 2014 Novel silicon surface passivation by Al_2O_3/ZnO/Al_2O_3 films deposited by thermal atomic layer deposition *Japan. J. Appl. Phys.* **53** 04ER19

[41] Suh D and Weber K 2014 Effective silicon surface passivation by atomic layer deposited Al_2O_3/TiO_2 stacks *Phys Status Solidi*—R **8** 40–3

[42] Wang W C *et al* 2013 Surface passivation of efficient nanotextured black silicon solar cells using thermal atomic layer deposition *ACS Appl. Mater. Interfaces* **5** 9752–9

[43] Benick J, Hoex B, van de Sanden M C M, Kessels W M M, Schultz O and Glunz S W 2008 High efficiency n-type Si solar cells on Al_2O_3-passivated boron emitters *Appl. Phys. Lett.* **92** 253504

[44] Hoex B, Schmidt J, Pohl P, van de Sanden M C M and Kessels W M M 2008 Silicon surface passivation by atomic layer deposited Al_2O_3 *J. Appl. Phys.* **104** 44903

[45] Li K T, Wang X Q, Lu P F, Ding J N and Yuan N Y 2014 Influence of the microstructure of n-type Si : H and passivation by ultrathin Al_2O_3 on the efficiency of Si radial junction nanowire array solar cells *Sol. Energy Mater Sol. Cells* **128** 11–7

[46] Lee B G, Li S, von Gastrow G, Yli-Koski M, Savin H, Malinen V, Skarp J, Choi S and Branz H M 2014 Excellent passivation and low reflectivity with atomic layer deposited bilayer coatings for n-type silicon solar cells *Thin Solid Films* **550** 541–4

[47] Wu Y Z *et al* 2014 Highly compact TiO_2 layer for efficient hole-blocking in perovskite solar cells *Appl. Phys. Express* **7** 052301

[48] Poodt P, Lankhorst A, Roozeboom F, Spee K, Maas D and Vermeer A 2010 A high-speed spatial atomic-layer deposition of aluminum oxide layers for solar cell passivation *Adv. Mater.* **22** 3564–8

[49] Hu S, Shaner M R, Beardslee J A, Lichterman M, Brunschwig B S and Lewis N S 2014 Amorphous TiO_2 coatings stabilize Si, GaAs, and GaP photoanodes for efficient water oxidation *Science* **344** 1005–9

[50] Paracchino A, Laporte V, Sivula K, Grätzel M and Thimsen E 2011 Highly active oxide photocathode for photoelectrochemical water reduction *Nat. Mater.* **10** 456–61

[51] Chen Y W, Prange J D, Dühnen S, Park Y, Gunji M, Chidsey C E D and McIntyre P C 2011 Atomic layer-deposited tunnel oxide stabilizes silicon photoanodes for water oxidation *Nat. Mater.* **10** 539–44

[52] Lee M H *et al* 2012 p-type InP panopillar photocathodes for efficient solar-driven hydrogen production *Angew. Chem., Int. Ed. Engl.* **51** 10760–4

[53] Vannucci A K, Alibabaei L, Losego M D, Concepcion J J, Kalanyan B, Parsons G N and Meyer T J 2013 Crossing the divide between homogeneous and heterogeneous catalysis in water oxidation *Proc. Natl. Acad. Sci. USA* **110** 20918–22

[54] Sivula K, Le F F and Grätzel M 2011 Solar water splitting: progress using hematite (α-Fe_2O_3) photoelectrodes *ChemSusChem* **4** 432–49

[55] Bassi P S, Gurudayal, Wong L H and Barber J 2014 Iron based photoanodes for solar fuel production *Phys. Chem. Chem. Phys.* **16** 11834–42

[56] Beermann N, Vayssieres L, Lindquist S E and Hagfeldt A 2000 A photoelectrochemical studies of oriented nanorod thin films of hematite *J. Electrochem. Soc.* **147** 2456–61

[57] Xi L, Chiam S Y, Mak W F, Tran P D, Barber J, Loo S C J and Wong L H 2013 A novel strategy for surface treatment on hematite photoanode for efficient water oxidation *Chem. Sci.* **24** 164–9

[58] Le Formal F, Tetreault N, Cornuz M, Moehl T, Gratzel M and Sivula K 2011 Passivating surface states on water splitting hematite photoanodes with alumina overlayers *Chem. Sci.* **2** 737–43

[59] Xi L, Bassi P S, Chiam S Y, Mak W F, Tran P D, Barber J, Chye Loo J S and Wong L H 2012 Surface treatment of hematite photoanodes with zinc acetate for water oxidation *Nanoscale* **4** 4430–3

[60] Xi L, Tran P D, Chiam S Y, Bassi P S, Mak W F, Mulmudi H K, Batabyal S K, Barber J, Loo J S C and Wong L H 2012 Co_3O_4-Decorated hematite nanorods as an effective photoanode for solar water oxidation *J. Phys. Chem.* C **116** 13884–9

[61] Brennan T P, Ardalan P, Lee H B R, Bakke J R, Ding I K, McGehee M D and Bent S F 2011 Atomic layer deposition of CdS quantum dots for solid-state quantum dot sensitized solar cells *Adv. Energy Mater.* **1** 1169–75

[62] Dasgupta N P, Jung H J, Trejo O, McDowell M T, Hryciw A, Brongersma M, Sinclair R and Prinz F B 2011 Atomic layer deposition of lead sulfide quantum dots on nanowire surfaces *Nano Lett.* **11** 934–40

[63] Sarkar S K, Kim J Y, Goldstein D N, Neale N R, Zhu K, Elliot C M, Frank A J and George S M 2010 In_2S_3 atomic layer deposition and its application as a sensitizer on TiO_2 nanotube arrays for solar energy conversion *J. Phys. Chem.* C **114** 8032–9

[64] Luo J, Karuturi S K, Liu L, Su L T, Tok A I Y and Fan H J 2012 Homogeneous photosensitization of complex TiO_2 nanostructures for efficient solar energy conversion *Sci. Rep.* **2** 451–6

[65] Su L T *et al* 2013 Photon upconversion in hetero-nanostructured photoanodes for enhanced near-infrared light harvesting *Adv. Mater.* **25** 1603–7

[66] Dasgupta N P, Liu C, Andrews S, Prinz F B and Yang P D 2013 Atomic layer deposition of platinum catalysts on nanowire surfaces for photoelectrochemical water reduction *J. Am. Chem. Soc.* **135** 12932–5

[67] Dai P C, Xie J, Mayer M T, Yang X G, Zhan J H and Wang D W 2013 Solar hydrogen generation by silicon nanowires modified with platinum nanoparticle catalysts by atomic layer deposition *Angew. Chem., Int. Ed. Engl.* **52** 11119–23

[68] Baxter J B and Aydil E S 2005 Nanowire-based dye-sensitized solar cells *Appl. Phys. Lett.* **86** 53114–20

[69] Liu L, Karuturi S K, Su L T and Tok A I Y 2011 TiO_2 inverse-opal electrode fabricated by atomic layer deposition for dye-sensitized solar cell applications *Energy Environ. Sci.* **4** 209–15

[70] Ryan M 2009 Progress in ruthenium complexes for dye sensitised solar cells *Platinum Met. Rev.* **53** 216–8

[71] Törndahl T, Platzer-Björkman C, Kessler J and Edoff M 2007 Atomic layer deposition of $Zn_{1-x}Mg_xO$ buffer layers for Cu(In,Ga)Se_2 solar cells *Prog. Photovolt., Res. Appl.* **15** 225–35

[72] Naghavi N *et al* 2013 Buffer layers and transparent conducting oxides for chalcopyrite Cu(In,Ga)$(S,Se)_2$ based thin film photovoltaics: present status and current developments *Prog. Photovolt., Res. Appl.* **18** 411–33

[73] Delft J A, Garcia-Alonso D and Kessels W M M 2012 Atomic layer deposition for photovoltaics: applications and prospects for solar cell manufacturing *Semicond. Sci. Technol.* **27** 74002

[74] Platzer-Björkman C, Törndahl T, Abou-Ras D, Malmström J, Kessler J and Stolt L 2006 Zn(O,S) buffer layers by atomic layer deposition in Cu(In,Ga)Se_2 based thin film solar cells: Band alignment and sulfur gradient *J. Appl. Phys.* **100** 44506

[75] Zimmermann U, Ruth M and Edoff M 2006 Cadmium-free CIGS mini-modules with ALD-grown Zn (O,S)-based buffer

layers *Proc. of 21st European Photovoltaic Solar Energy Conf.* pp 1831–4

[76] Kobayashi T, Kumazawa T, Jehl L K Z and Nakada T 2013 Cu(In,Ga)Se_2 thin film solar cells with a combined ALD-Zn(O,S) buffer and MOCVD-ZnO : B window layers *Sol. Energy Mater. Sol. Cells* **119** 129–33

[77] Merdes S, Malinen V, Ziem F, Lauermann I, Schule M, Stober F, Hergert F, Papathanasiou N and Schlatmann R 2014 Zn(O,S) buffer prepared by atomic layer deposition for sequentially grown Cu(In,Ga)$(Se,S)_2$ solar cells and modules *Sol Energy Mater. Sol. Cells* **126** 120–4

[78] Lindahl J, Wätjen J T, Hultqvist A, Ericson T, Edoff M and Törndahl T 2013 The effect of $Zn_{1-x}Sn_xO_y$ buffer layer thickness in 18.0% efficient Cd-free Cu(In,Ga)Se_2 solar cells *Prog. Photovolt., Res. Appl.* **21** 1588–97

[79] Hultqvist A, Platzer-Björkman C, Zimmermann U, Edoff M and Törndahl T 2012 Growth kinetics, properties, performance, and stability of atomic layer deposition Zn–Sn–O buffer layers for Cu(In,Ga)Se_2 solar cells *Prog. Photovolt., Res. Appl.* **20** 883–91

[80] Kapilashrami M, Kronawitter C X, Torndahl T, Lindahl J, Hultqvist A, Wang W C, Chang C L, Mao S S and Guo J 2012 Soft x-ray characterization of $Zn_{1-x}Sn_xO_y$ electronic structure for thin film photovoltaics *Phys. Chem. Chem. Phys.* **14** 10154–9

[81] Törndahl T, Coronel E, Hultqvist A, Platzer-Björkman C, Leifer K and Edoff M 2009 The effect of $Zn_{1-x}Mg_xO$ buffer layer deposition temperature on Cu(In,Ga)Se_2 solar cells: a study of the buffer/absorber interface *Prog. Photovolt., Res. Appl.* **17** 115–25

[82] Hultqvist A, Platzer-Björkman C and Törndahl T 2007 *22nd European Photovoltaic Solar Energy Conf. and Exhibition (Milan)*

[83] Abou-Ras D, Rudmann D, Kostorz G, Spiering S, Powalla M and Tiwari A N 2005 Microstructural and chemical studies of interfaces between Cu(In,Ga)Se_2 and In_2S_3 layers *J. Appl. Phys.* **97** 084908

[84] Naghavi N, Spiering S, Powalla M, Cavana B and Lincot D 2003 High-efficiency copper indium gallium diselenide (CIGS) solar cells with indium sulfide buffer layers deposited by atomic layer chemical vapor deposition (ALCVD) *Prog. Photovolt., Res. Appl.* **11** 437–43

[85] Sterner J, Malmström J and Stolt L 2005 Study on ALD In_2S_3/Cu(In,Ga)Se_2 interface formation *Prog. Photovolt., Res. Appl.* **13** 179–93

[86] Spiering S, Hariskos D, Schröder S and Powalla M 2005 Stability behaviour of Cd-free Cu(In,Ga)Se_2 solar modules with In_2S_3 buffer layer prepared by atomic layer deposition *Thin Solid Films* **480** 195–8